

DEVELOPMENT OF SILICON CARBIDE HEAT-RESISTANT COMPOSITES WITH MICRO-POROUS STRUCTURE

Kazuaki NISHIYABU*, Satoru MATSUZAKI**, Masaki KOTANI***

[Kazuaki NISHIYABU]: kazu@ipc.osaka-pct.ac.jp

*Osaka Pref. Col. of Tech., **Taisei Kogyo Co., ***Japan Aerospace Exploration Agency

Keywords: *silicon carbide, porous structure, space holder method, pyrolysis process*

1 Introduction

One of the causes that interferes with the future development of a re-usable space transportation system is the aerodynamic heating phenomenon which causes damage to its airframe during re-entry [1,2]. Thus heat-resistant composite materials with higher mechanical properties and reliability are required. Silicon carbide (SiC) has superior characteristics as a structural material from the viewpoints of mechanical properties at high temperature and chemical stability. However, because SiC has very brittle characteristic, fiber reinforcement is needed to improve the fracture toughness. There have been many efforts on the process development of SiC fiber reinforced SiC composite materials [3-18]. One of the most promising candidate methods is the polymer impregnation and pyrolysis (PIP) process as shown in Fig.1. This however has to be improved for reducing initial defects, i.e., internal cracks and voids formed in processing as shown in Fig.2.

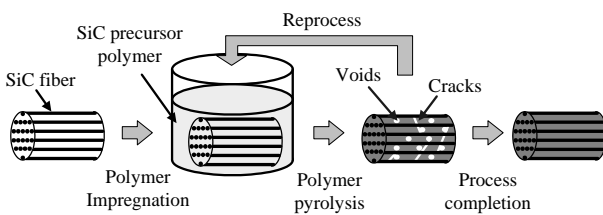


Fig.1 Production of SiC/SiC composite materials by conventional PIP process.

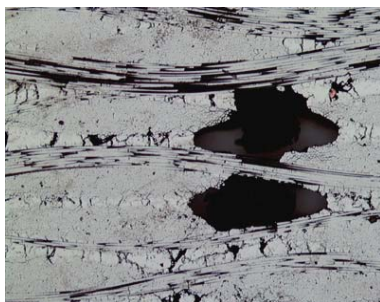


Fig.2 Internal defects of SiC/SiC composite materials produced by conventional PIP process.

In the conventional PIP process, it is difficult to degas during polymer pyrolysis, and also to disperse the shrinkage in polymer curing and pyrolysis. This study was attempted to reduce the initial defects in PIP processing by introducing a micro-porous structure in the SiC matrix. Though the final aim of this study is to obtain the sound SiC fiber reinforced SiC composite materials, the material combinations and production conditions of sound SiC porous matrix were also investigated in this paper. Using the optimum materials and processing conditions for SiC porous matrix, attempts to produce SiC fiber reinforced SiC porous composites were made. Furthermore, SiC fiber reinforced SiC dense matrix composites were produced by repeating the PIP process. The effectiveness of introducing the porous structure in PIP process was confirmed by evaluating the mechanical properties of SiC/SiC composites.

2 Fabrication Method of SiC/SiC Composites via Porous Structure

Some of the authors have developed a production method which can manufacture the micro-porous metal components with a high accuracy and complex shapes using most kinds of metal powder [19]. In order to form the porous structure with an arbitrary specified pore size and porosity, the polymethylmethacrylate (PMMA) particle is used to make spherical spaces in metal powders as shown in Fig.3. The key point of the pore formation process named powder space holder (PSH) method is to remove a large amount of PMMA particles from brittle compacts and to obtain many spaces surrounded by metal powders. This has been achieved by applying the polymer-debinding technique based on metal powder injection molding (MIM) process which is a manufacturing method combining traditional powder metallurgy (P/M) with plastic injection molding as shown in Fig.4 [20].

In this study, the micro-porous structure was introduced to aim reducing predominant defects which occur in the firing process of SiC precursor polymer. The PSH method was applied to PIP process as shown in Fig.5. Space holding particles were mixed into SiC precursor polymer and were removed by thermal pyrolysis to form a porous structure. Finally the porous matrix was densified by re-impregnation and pyrolysis of SiC precursor polymer.

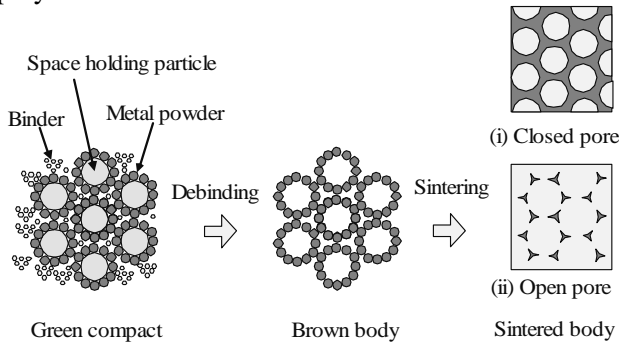


Fig.3 Flow of powder space holder method for producing micro-porous metals [19].

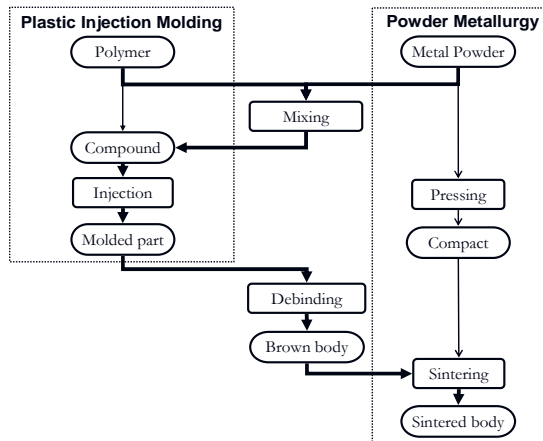


Fig.4 Flow of metal injection molding (MIM) process and characteristic polymer-debinding technique.

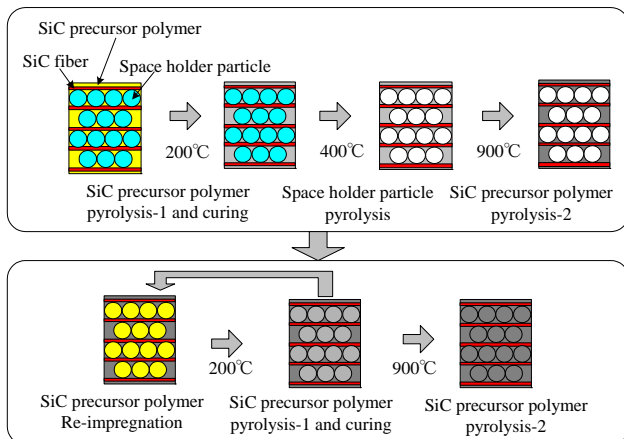


Fig.5 Production of SiC porous and SiC/SiC composite materials by applying PSH method into PIP process.

3 Materials and Experimental Conditions

The experimental materials used in this study are listed in Table 1. The polymer used for the SiC matrix precursor is allyl-hydride-polycarbosilane (AHPCS, Starfire Systems Inc., STARFIRE SMP-10). The yield of AHPCS is comparably high as 68wt.%. Two kinds of poly-methyl-methacrylate (PMMA) particles were used for space holding material. Their mean diameters and specific tap densities are 10 μ m, 45vol.% (Soken Chemical & Engineering Co., Ltd., Chemi-Snow MX-1000) and 90 μ m, 64vol.% (GANZ Chemical Co., Ltd., Ganz-Pearl GM9005), respectively. Two kinds of textiles made from SiC fiber were used for the reinforcement of SiC matrix; 1) Nonwoven fabric made from SiC fiber (Ube-Industries Co., Ltd., Tyranno[®] ZMI-SIE08PX), 2) Unidirectional fiber (Ube-Industries Co., Ltd., Tyranno[®] PM-S17E08PX). Both the fibers were coated with C layer (300nm) and SiC layer (100nm) by chemical vapor infiltration (CVI). Due to the easy degassing, open porous structure is preferable to reduce the defects formed during pyrolysis. Open porous structures form when the PMMA particles are in contact with each other. In this study, the effects of material condition on porous structure were investigated by changing several main fractions of PMMA particle based on the relative tap densities as shown in Fig.6. Tap density, T.D. (g/cm³) is determined by applying a controlled packing force to the powder. In the packing state, the powder particles are interconnected with each other. Relative tap density, R.T.D. (%) is a measure of the tap density divided by the true density. In order to study the micro-structural evolution by heating, the samples that are heated to a temperature just before remarkable weight decrease are subjected to observation. The shrinkage rates of the samples were also evaluated by measuring the dimensions to assess dimensional stability and micro-structural evolution mechanism.

Table 1 Experimental materials

Materials	Composition	Producer	Product ID
SiC precursor polymer	-SiHR-CH ₂ -(AHPCS)	Strrarfire systems Inc.	SMP-10
Space holder particle	Poly-methyl-methacrylate (PMMA)	Soken Chemical Co., Ltd.	10 μ m (MX100)
		Ganz Chemical Co., Ltd.	90 μ m (GM9005)
SiC fiber Nonwoven	SiC	Ube-Industries Co., Ltd.	Tyranno [®] ZMI-SIE08PX
SiC fiber UD	SiC	Ube-Industries Co., Ltd.	Tyranno [®] ZMI-SIE08PX

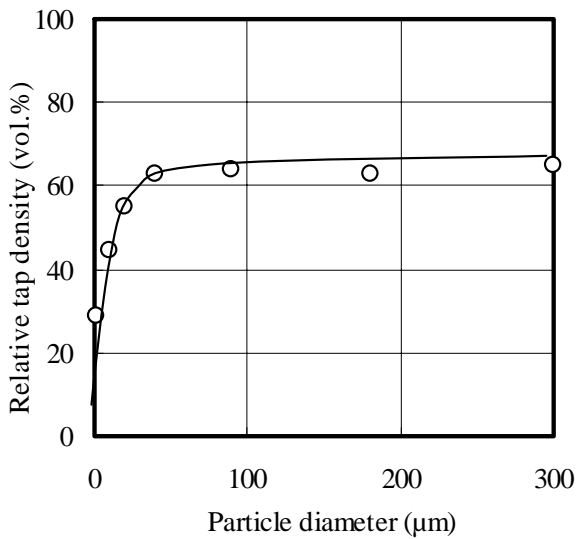


Fig.6 Relative tap density of PMMA particle as function of the particle diameter.

4 Results and Discussions

4.1 Curing and Pyrolysis Behaviors

To design the suitable firing condition, the curing behavior of AHPCS polymer and the pyrolysis behavior of AHPCS polymer and PMMA particle were evaluated by rotational-rheometer and thermo-gravimeter, respectively. The results are shown in Fig.7 and Fig.8. Fig.7 reveal that AHPCS polymer is cured rapidly at 130°C and almost cured at 230°C. Fig.8 shows that the weight loss in pyrolysis of AHPCS polymer is obviously seen at two steps; 1) 60~200°C and 2) 420~900°C, while PMMA particle is decomposed from 190°C to 420°C.

These measurement results suggest that there are two steps of decomposition mechanisms as follows. Firstly in lower temperature below 420°C, AHPCS polymer solidified with pyrolytically decomposing of 13% in weight. Thus it makes the paths for pyrolysis gassing around PMMA particles incompletely-decomposed. This seemed to be a most important effect to form soundly the brittle polymeric green body with micro-porous structure. This concept can be achieved by applying the original polymer-debinding technique in PSH method based on MIM process. Secondly in higher temperature over 420°C, PMMA particles have been removed completely and the porous structure was formed in AHPCS monoliths. In such a porous structure suitable for degassing, AHPCS polymer decomposes continuously to 35% in weight.

Consequently, it seems that these sequences of pyrolysis are quite preferable for realizing an effective gas purge to obtain more sound polymeric green body with uniform shrinkage. Thus in this study, the heating schedule as shown in Fig.9 is specified. The extremely slow heating rate from room temperature to 400°C is chosen to avoid an undesirable crack due to pyrolysis-gassing and differential shrinkage. This heating rate and vacuum degassing process should be considered when a large amount of PMMA particles is used. Over 400°C, the comparatively high heating rate to 900°C is applied.

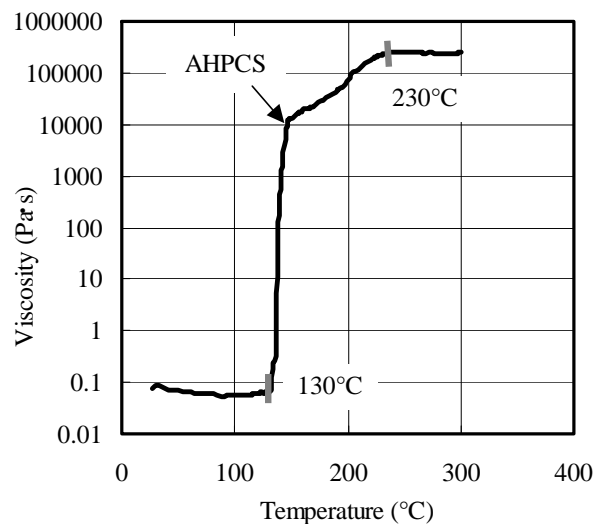


Fig.7 Change in viscosity of AHPCS polymer.

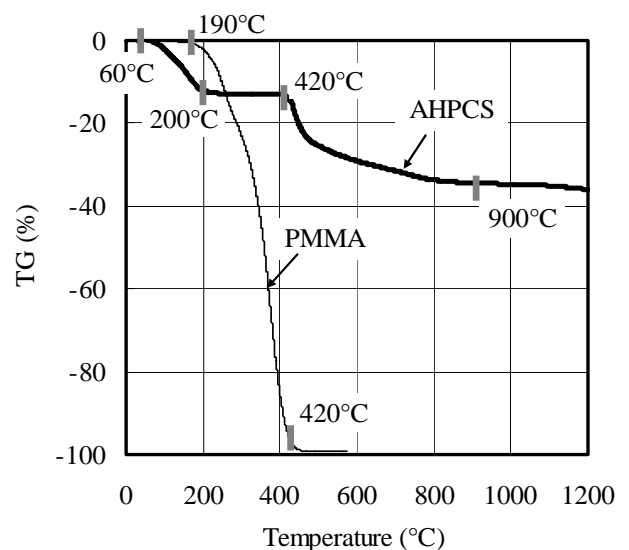


Fig.8 Thermal gravimetric curves of AHPCS polymer and PMMA particle.

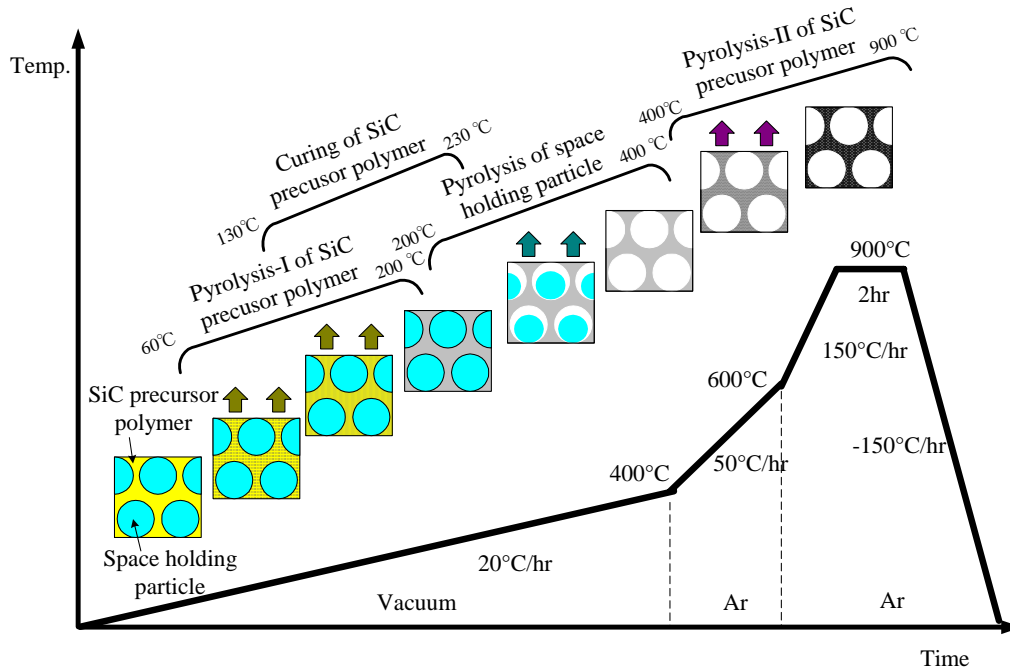


Fig.9 Formation mechanism of SiC porous structure by PSH-PIP method and heating conditions used for experiments.

4.2 Defects in Curing and Pyrolysis of SiC Precursor Polymer

The problem begun with curing and low temperature pyrolysis of plain AHPCS polymer was investigated. The pictures and schematic drawings of AHPCS polymer specimens with various thicknesses processed at 200°C are shown in Fig.10. There were voids and obvious cracks in the specimens with over $t=3\text{mm}$ thick. This seems to be due to a hard degassing and a differential shrinkage in pyrolysis and curing of AHPCS polymer. Thin specimens ($t=2\text{mm}$) without defects in processing at 200°C were heated at 900°C. The SEM image is shown in Fig.11. Many microscopic cracks occurred on the surface are seen. These evidences provide a fact that it is very difficult to make a bulky specimen using plain AHPCS polymer. It is also projected that any defects is likely to occur in the parts of rich AHPCS polymer (over 2mm in size).

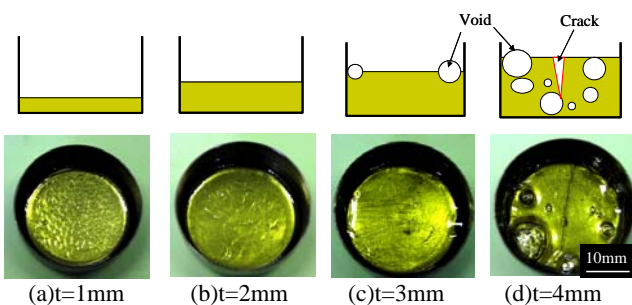


Fig.10 Effects of thickness on defects of AHPCS polymer processed at 200°C.

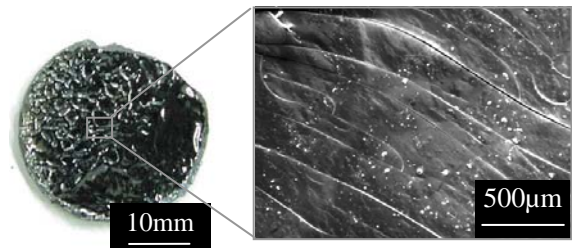
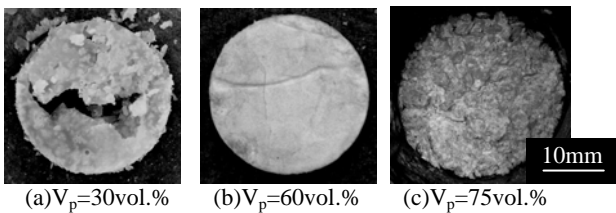


Fig.11 Microscopic cracks occurred on surface of AHPCS polymer ($t=2\text{mm}$) processed at 900°C.

4.3 Low Temperature Pyrolysis Behaviors of SiC Precursor Polymer with Space Holding Particles

By adding PMMA particle in AHPCS polymer, the changes such as an increase in viscosity at room temperature and the loss of shape after decomposing AHPCS polymer were affected significantly. The effects of size and volume fraction of PMMA particle added in AHPCS polymer on shape retention were investigated. Fig. 12 shows the appearances of disk specimens with various volume fractions of PMMA particle ($d_p=10\mu\text{m}$) processed at 200°C. In case of specimen with lower volume fraction of PMMA particle ($V_p=30\text{vol.}\%$), there is a large crack in the center of the specimen. This is due to a hard degassing and a differential shrinkage in pyrolysis and curing of AHPCS polymer as described in section 4.2. This means that there are no positive effects by adding such a lower fraction of PMMA particle. In case of specimen with intermediate volume fraction of PMMA particle

($V_p=60\text{vol.}\%$), on the other hand, a disk specimen without defects in appearance was obtained. It seems that a decreasing in amount of degassing AHPCS polymer by adding PMMA particle acted effectively on reduced voids and cracking. However, in case of specimen with higher volume fraction of PMMA particle ($V_p=75\text{vol.}\%$), it is impossible to maintain the form. This is due to an insufficient amount of compact because PMMA particle are over closely-packed.



(a) $V_p=30\text{vol.}\%$ (b) $V_p=60\text{vol.}\%$ (c) $V_p=75\text{vol.}\%$
 Fig.12 Appearances of disk specimens with various volume fractions of PMMA particle ($d_p=10\mu\text{m}$) processed at 200°C .

Further investigations were carried out more extensively by changing the size and volume fraction of PMMA particle. The results are summarized in process mapping for various combinations of PMMA particle as shown in Fig.13. In specimens with any sizes of PMMA particle, sound disk specimens without damages were obtained by adding PMMA particle around $V_p=60\text{--}70\text{vol.}\%$. However, in the area-A with adding too much PMMA particle, it is impossible to mix the materials. In contrast, with the area-B, internal voids occurred due to hard degassing and a differential shrinkage in pyrolysis and curing of AHPCS polymer with less PMMA particle. Also, in the area-C, microscopic-cracking become a significant defect. In the area-D, it is impossible to make the rigid form.

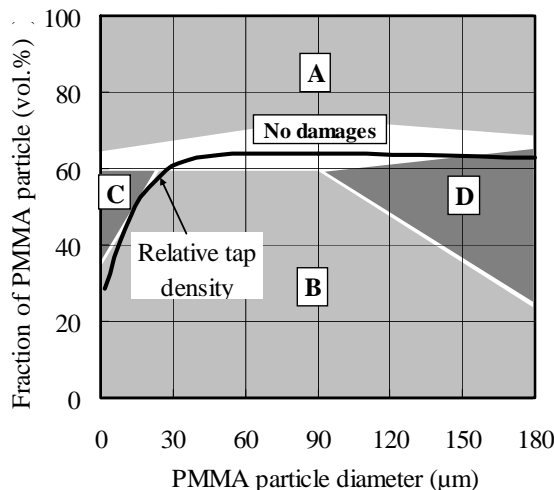


Fig.13 Effect of PMMA mixture condition on defects.

Thus roughly speaking, it is concluded that the suitable combinations of PMMA particle are related to the relative tap density of PMMA particle. The preferable volume fraction of PMMA particle is an equivalent amount of relative tap density for each size of PMMA particle as rule-of-thumb. These selections of materials are useful only for making the form before removing the PMMA particles, and then will be considered again in the next section.

4.4 Shape Retention of SiC Porous Structured Body after Firing

The effects of size and volume fraction of PMMA particle added in AHPCS polymer on shape retention after removing PMMA particles were investigated. The appearances of specimens fired at 400°C with various combinations in size and fraction of PMMA particle are shown in Fig.14. In the specimens fabricated under the condition of relative tap density of PMMA particle and below, many destructive large cracks were formed on the surface as shown in Fig.14(a)(b)(d) and (e). The crack disappeared in the condition of higher relative tap density of PMMA particle as shown in Fig.14(c) and (f).

Those reasons are explained by schematic drawings shown in Fig.15. Fig.15(a) shows pyrolysis process of plain AHPCS polymer without adding PMMA particle. As described in section 4.2, large cracks occurred due to a hard degassing and a differential shrinkage in pyrolysis and curing of AHPCS polymer. In Fig.15(b) where volume fraction of PMMA particle is below relative tap density, PMMA particles deposit at the bottom of the specimen. Consequently cracks were formed at the upper part of AHPCS solid as case of plain AHPCS polymer shown in Fig.15(a). On the other hand, in Fig.15(c) where volume fraction of PMMA is above relative tap density, PMMA particles distributed across the specimens. In this condition, an effective degassing and a stable shrinkage can occur. However, in a much higher fraction of PMMA particle, it is difficult to retain a shape because of the lack of formation agent.

Thus, the above-mentioned results suggest that it is necessary for fabricating of sound SiC porous body to select the combination in size and volume fraction of PMMA particle where the rich parts of AHPCS polymer are not formed, i.e. PMMA particles are closely-packed in AHPCS polymer and pyrolysis gas is likely to evacuate from inside to outside.

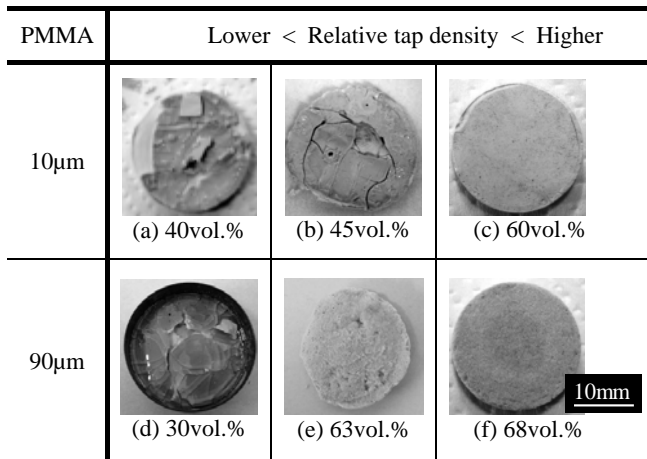


Fig.14 Effects of volume fraction and size of PMMA particle on the shape retention of AHPCS polymer with PMMA particles processed at 400°C.

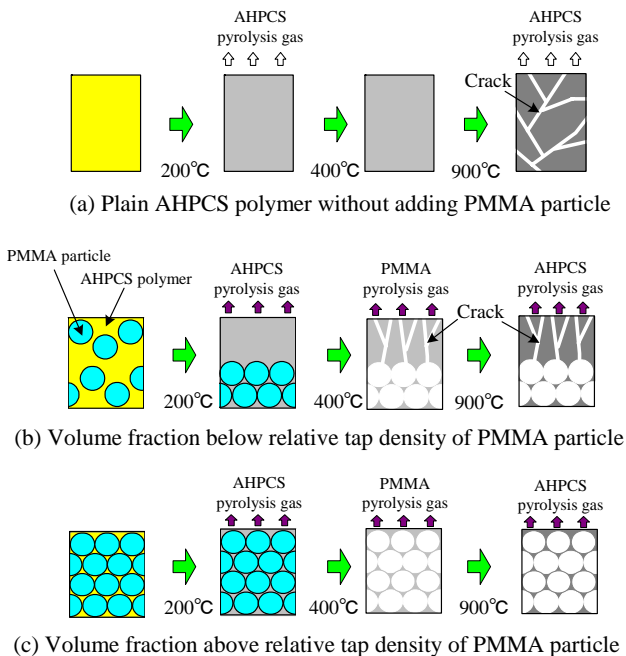


Fig.15 Pyrolysis behavior of specimens with varied volume fractions of PMMA particle.

Fig.16 shows the available condition area of the size and volume fraction of PMMA particle. In the area-A, it is inapplicable because of the lack of uniform dispersion of the particle due to insufficient fluidity. In contrast, in the area-B, it is also inapplicable because of insufficient function of the particle, which results in a large amount of void formation during pyrolysis. Also, in the area-C, it is not suitable because of significant defect formation. In area-D and area-E which are not listed under this experiment, it is predicted to involve a difficult operation in mixing and to form a coarser shape, respectively.

This is similar as the result shown in Fig.13, and shape retention of SiC porous structure after firing is affected significantly by the shape conditions after the pyrolysis at lower temperature. As a result, it is shown that the applicable volume fraction of PMMA particle is 60-63 vol.% for 10μm and 60-70 vol.% for 90μm in diameter of PMMA particle.

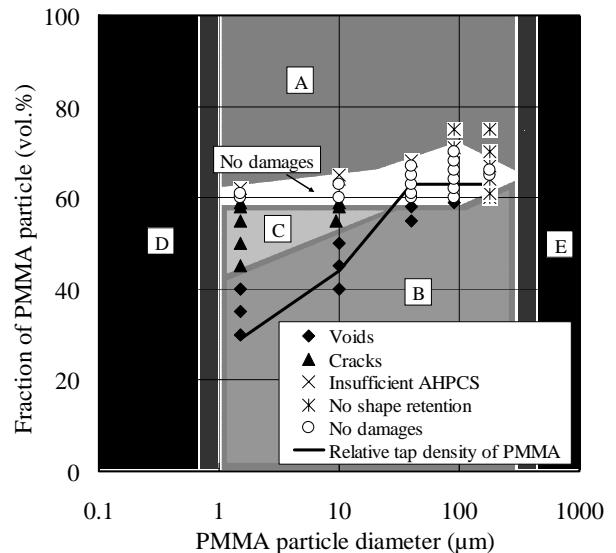


Fig.16 Production possibility area of SiC porous structure.

4.5 Microstructures and Properties of SiC Porous Body

The specimens for which the shape retention was successfully achieved at 400°C were successively fired up to 900°C. Fig.17 shows a representative microstructure of the specimens. It was found that the porous structures with open spherical shaped pores were uniformly formed. The pore size is dependent on the diameter of PMMA particle used. Furthermore, a homogeneous microporous bulky SiC body without any defects was successfully obtained as shown in Fig.18. Such large and thick specimens have never been fabricated by conventional polymeric process techniques.

This result confirmed the effectiveness of porous structure in shape retention of SiC body fabricated with polymer precursor. There is a clear possibility that larger size of porous specimen can be fabricated by applying such a micro-porous structure and this porous body can be densified by repeating a re-polymer impregnation and pyrolysis process.

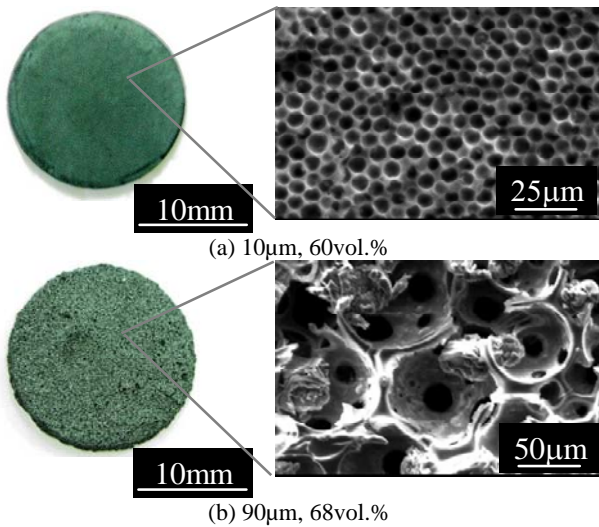
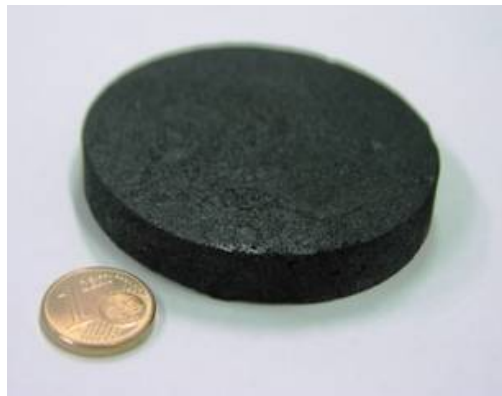
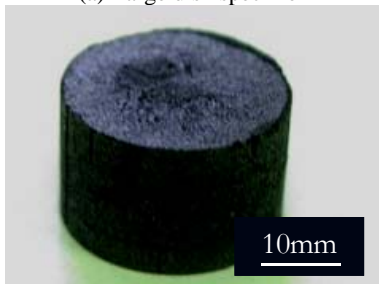


Fig.17 Microstructures of SiC porous materials fabricated by using a different size of PMMA particle.



(a) Large disk specimen

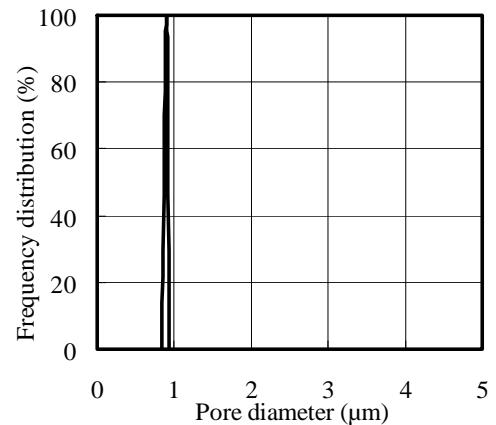


(b) Thick cylindrical specimen

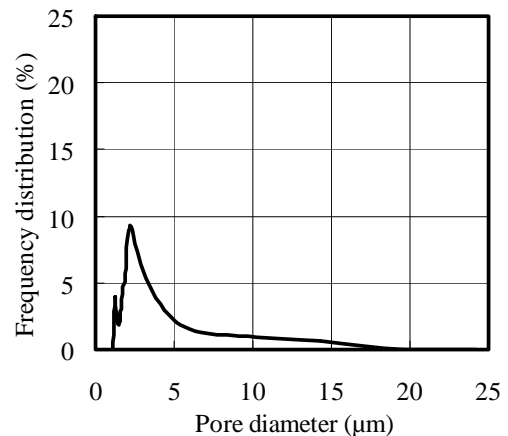
Fig.18 Examples of bulky SiC porous specimen fabricated by using PMMA particle of 90µm, 68vol.%.

The pore size, the pore distribution and the surface area were measured with a porometer (PMI, CPF-1100-AXLSP) with which the flow resistance of a fluid through the porous sample can be measured. The porosity and the shrinkage of the specimens were measured with micrometer calipers and an analytical balance. Fig.19 shows the pore size distributions of SiC porous specimens fabricated by using (a) small PMMA particle (10µm, 60vol.%) and (b) large PMMA particle (90µm, 68vol.%). Also, the measurement results are

summarized in Table 2. When 10µm PMMA particle is used, the sharp peak is shown at 0.90µm, corresponding to the interconnected pores shown in Fig.17(a). While 90µm PMMA particle is used, the pore size is distributed broadly around 3µm, reflecting to the morphological appearance of Fig.17(b). On the other hand, the porosity is higher than the volume fraction of PMMA particle added. This means there are voids and cracks around the pores. It is a natural result that the specific surface area is higher in specimens with smaller pore size which were fabricated by using small PMMA particle.



(a) In small PMMA particle (10µm, 60vol.%)



(b) In large PMMA particle (90µm, 68vol.%)

Fig.19 Pore size distributions of SiC porous specimens.

Table 2 Summary of properties of SiC porous specimens

	Size and volume fraction of PMMA particle	
	10µm, 60vol.%	90µm, 68vol.%
Porosity	74.8%	88.4%
Mean pore size (Narrowest portion of interconnected pore)	0.90µm	4.33µm
Specific surface area	3.55m ² /g	0.455m ² /g

Fig.20 shows the shrinkage percentage of porous specimens as the function of volume fraction of PMMA particles. In both specimens fabricated by using 10 μ m and 90 μ m PMMA particle, the shrinkage percentage decreases linearly as the volume fraction of PMMA particle decreases. To reduce cracks, lowering the shrinkage is required. Thus large PMMA particle is preferable in composite fabrication.

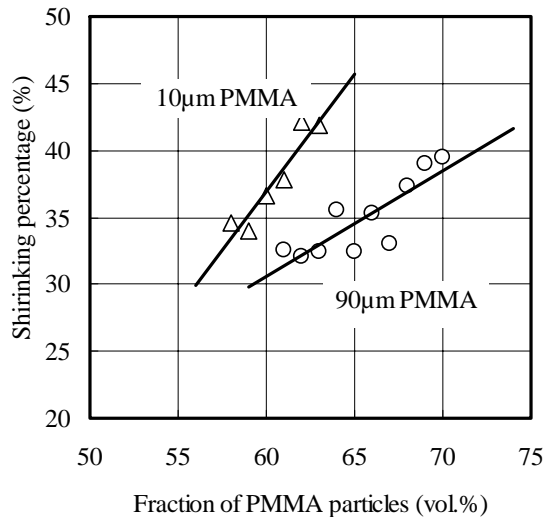


Fig.20 Shrinkage percentage vs. fraction of PMMA particles.

4.6 SiC Fiber Reinforcement to SiC Porous Body

The fabrication of a composite by PSH-PIP process was attempted. As a trial study, SiC felt with an isotropic non-woven structure made from short fiber was used, because the rigid fiber disturbs a shrinkage of AHPCS polymer in firing and is at high risk of destruction. Fig.21 and Fig.22 shows SEM images of cross-sections of SiC fiber reinforced SiC dense matrix composites without PMMA particles and SiC porous matrix fabricated using 10 μ m, 45vol.% of PMMA particle, respectively. As shown in Fig.21, the fibers are dispersed in SiC dense matrix, but the body breaks into blocks. The fiber provides more destructive damage than the specimens fired by plain AHPCS polymer without fibers. As generally recognized, a fiber reinforcement of the brittle matrix fabricated by firing process can not be achieved easily. In SiC porous matrix, on the other hand, there are a huge number of micro-sized pores around the fibers and also loose slippery interfaces around un-reacted fibers as shown in Fig.22. Owing to this preliminary study, some advantage of our approach can be found.

Material selection guide to be considered for fiber reinforcement is shown in Fig.23. To make a

homogeneous porous body of non-destructive cracks, higher volume fraction and smaller size of PMMA particle are preferable. However it is undesirable to use a large amount of PMMA particle in the view point of its viscosity. Thus the volume fraction of PMMA particle should be carefully selected to satisfy the requirements in viscosity and pyrolyzed matrix's integrity. There is some creative strategy i. e. 1) partly squeezing out a polymer, which increases the volume fraction of PMMA particle after impregnation, 2) using a spreadable fibrous tape and so on.

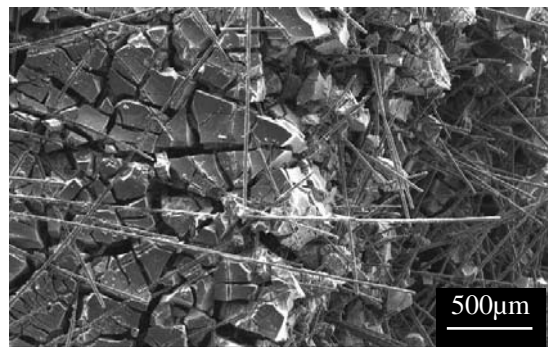


Fig.21 SEM images of cross-sections of SiC fiber reinforced SiC dense matrix composites without PMMA particles.

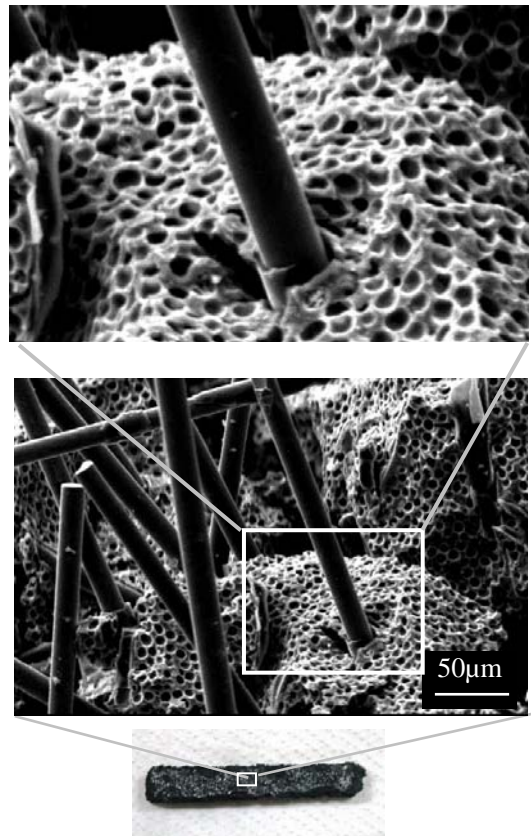


Fig.22 SEM images of cross-sections of SiC fiber reinforced SiC porous matrix composites (10 μ m, 45vol.% PMMA particle).

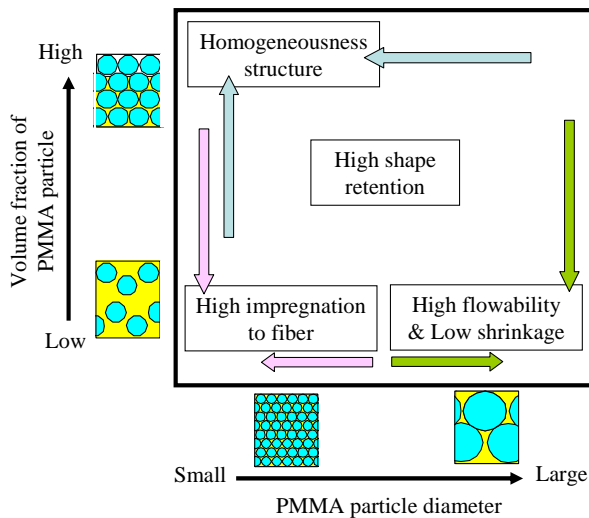


Fig.23 Material selection guide to be considered for fiber reinforcement.

5 Application to Unidirectional SiC Fiber Reinforced SiC Composites

5.1 Fabrication Method and Process Conditions

The fabrication process of unidirectional SiC fiber reinforced SiC composites by PSH-PIP method is shown in Fig.24. Basically this is a liquid forming with bagging and is similar in process to the fiber reinforced polymeric matrix composites such as VaRTM process before firing. However, the viscosity of AHPCS polymer mixed with a large amount of PMMA particles is high, thus polymer impregnation to unidirectional SiC fiber was carried out by a dipping process. After firing at 900°C, re-polymer impregnation and pyrolysis process was applied 7 times in to total densify the porous matrix.

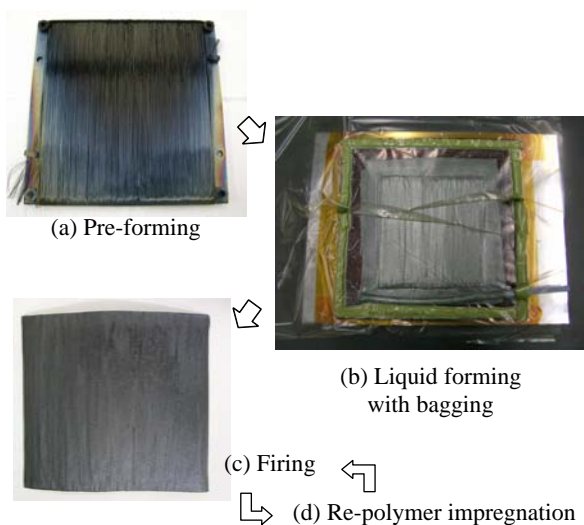
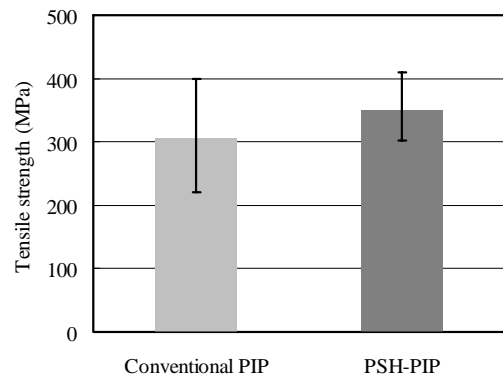


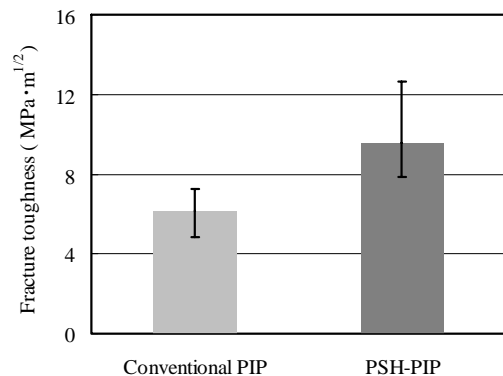
Fig.24 Fabrication process of unidirectional SiC fiber reinforced SiC composites.

5.2 Mechanical properties

Tensile strength and fracture toughness of unidirectional SiC fiber reinforced SiC composites fabricated by conventional PIP and PSH-PIP method are shown in Fig.25. Compared with the conventional PIP, the mechanical properties of PSH-PIP method were actually improved 14.2% in mean tensile strength and 54.9% in mean fracture toughness. The effectiveness of the route to matrix densification via porous structure was proven.



(a) Tensile strength



(b) Fracture toughness

Fig.25 Comparison of unidirectional SiC fiber/SiC matrix composites produced by conventional PIP and PSH-PIP method.

6 Conclusions

The adoption of PSH method into PIP process was proposed to reduce predominant defects formed in the firing process of SiC precursor polymer. Consequently, SiC porous materials and the fibrous composite materials with homogeneous open porous structure were successfully obtained without significant cracks. This is surely due to an efficient gas purge and a stable shrinkage by introducing the micro-porous structure in SiC matrix. By adopting this technique to composite fabrication, remarkable improvement of matrix integrity can be expected.

Acknowledgement

This study has been carried out as a part of R&D of Open Lab. Program operated by Japan Aerospace Exploration Agency (JAXA) and authors would like to acknowledge to all concerned for the foundations, and also to Mr. Yuki Futahashi and Mr. Tetsuya Ono, former students of Osaka Prefectural College of Technology for their experimental works.

References

- [1] Schmidt S., Beyer S., Knabe H., Immich H., Meistring R. and Gessler A., Advanced ceramic matrix composite materials for current and future propulsion technology applications, *Acta Astronautica*, Vol.55, Issues 3-9, New Opportunities for Space, Selected Proceedings of the 54th International Astronautical Federation Congress, pp.409-420, 2004.
- [2] Baiocco P., Guedron S., Plotard P. and Moulin J., The Pre-X atmospheric re-entry experimental lifting body: Program status and system synthesis, *Acta Astronautica*, (In Press), 2007.
- [3] Levine S.R., Opila E.J., Halbig M.C., Kiser J.D., Singh M. and Salem J.A., Evaluation of ultra-high temperature ceramics for aeropropulsion use, *Journal of the European Ceramic Society*, Vol.22, Issues 14-15, pp.2757-2767, 2002.
- [4] Kimmel J., Miriyala N., Price J., More K., Tortorelli P., Eaton H., Linsey G. and Sun E., Evaluation of CFCC liners with EBC after field testing in a gas turbine, *Journal of the European Ceramic Society*, Vol.22, Issues 14-15, pp.2769-2775, 2002.
- [5] Brennan J.J., Interfacial characterization of a slurry-cast melt-infiltrated SiC/SiC ceramic-matrix composite, *Acta Materialia*, Vol.48, Issues 18-19, pp.4619-4628, 2000.
- [6] Krenkel W. and Berndt F., C/C-SiC composites for space applications and advanced friction systems, *Materials Science and Engineering: A*, Vol.412, Issues 1-2, International Conference on Recent Advances in Composite Materials, 5, pp.177-181, 2005.
- [7] Jones R.H. and Henager Jr.C.H., Subcritical crack growth processes in SiC/SiC ceramic matrix composites, *Journal of the European Ceramic Society*, Vol.25, Issue 10, Corrosion of Ceramic Matrix Composites, pp.1717-1722, 2005.
- [8] Naslain R., Design, preparation and properties of non-oxide CMCs for application in engines and nuclear reactors: an overview, *Composites Science and Technology*, Vol.64, Issue 2, pp.155-170, 2004.
- [9] Reznik B., Gerthsen D., Zhang W. and Huttinger K.J., Microstructure of SiC deposited from methyltrichlorosilane, *Journal of the European Ceramic Society*, Vol.23, Issue 9, pp.1499-1508, 2003.
- [10] Kuroda M.Y. and Kusaka K., Development status of the reusable high-performance engines with functionally graded materials, *Acta Astronautica*, Vol.50, Issue 7, pp.427-432, 2002.
- [11] Morscher G.N. and Cawley J.D., Intermediate temperature strength degradation in SiC/SiC composites, *Journal of the European Ceramic Society*, Vol.22, Issues 14-15, pp.2777-2787, 2002.
- [12] Prakash S., Budhani R.C. and Bunshah R.F., Development of thin film temperature sensors for high performance turbo-jet engines, *Materials Research Bulletin*, Vol.23, Issue 2, pp.187-195, 1988.
- [13] Muhlatzer, Handrick K. and Pfeiffer H., Development of a new cost-effective ceramic composite for re-entry heat shield applications, *Acta Astronautica*, Vol.42, Issue 9, pp.533-540, 1998.
- [14] Monteverde F. and Savino R., Stability of ultra-high-temperature ZrB₂-SiC ceramics under simulated atmospheric re-entry conditions, *Journal of the European Ceramic Society*, (In Press), 2007.
- [15] Hurwitz F.I., Gyekenyesi J.Z. and Conroy P.J., Polymer Derived Nicalon/Si-C-O Composites: Processing and Mechanical Behavior, *Ceram.Eng. Sci. Proc.* 10 [7-8] 750-763, 1989.
- [16] Tanaka T., Tamari N., Kondoh I. and Iwasa M., Fabrication and Evaluation of 3-Dimensional Tyranno Fiber Reinforced SiC Composites by Repeated Infiltration of Polycarbosilane, *J. Ceram. Soc. Japan*, 103 [1] pp.1-5, 1995.
- [17] Kotani M., Inoue T., Kohyama A., Katoh Y. and Okamura K., Effect of SiC Particle Dispersion on Microstructure and Mechanical Properties of Polymer-Derived SiC/SiC Composite, *Materials Science and Engineering*, A357, pp.376-385, 2003.
- [18] Kotani M., Katoh Y., Kohyama A. and Narisawa M., Fabrication and Oxidation-Resistance Property of Allylhydridopolycarbosilane-Derived SiC/SiC Composites, *Journal of the Ceramics Society of Japan*, 111 [5], pp.300-307, 2003.
- [19] Nishiyabu K., Matsuzaki S. and Tanaka S., Dimensional accuracy of micro-porous metal injection and extrusion molded components produced by powder space holder method". *Journal of the Japan Society of Powder and Powder Metallurgy*, Vol.53, No.9, pp.776-781, 2006 (in Japanese).
- [20] German R.M. and Bose A., Injection Molding of Metals and Ceramics, *Metal Powder Industries Federation (MPIF)*, 1997.